



This article appeared in a journal published by Elsevier. The attached copy is furnished to the author for internal non-commercial research and education use, including for instruction at the authors institution and sharing with colleagues.

Other uses, including reproduction and distribution, or selling or licensing copies, or posting to personal, institutional or third party websites are prohibited.

In most cases authors are permitted to post their version of the article (e.g. in Word or Tex form) to their personal website or institutional repository. Authors requiring further information regarding Elsevier's archiving and manuscript policies are encouraged to visit:

<http://www.elsevier.com/copyright>



ELSEVIER

Available online at www.sciencedirect.com

Zoologischer Anzeiger 248 (2010) 285–298

Zoologischer
Anzeigerwww.elsevier.de/jcz

Combining confocal laser scanning and transmission electron microscopy for revealing the mastax musculature in *Bryceella stylata* (Milne, 1886) (Rotifera: Monogononta)

E.F. Wilts*, D. Wulfken, W.H. Ahlrichs

Systematics and Evolutionary Biology, Department of Biology and Environmental Sciences, Carl von Ossietzky University Oldenburg, 26111 Oldenburg, Germany

Received 4 November 2009; received in revised form 26 November 2009; accepted 26 November 2009

Corresponding Editor: Sorensen

Abstract

The rotiferan jaw apparatus (mastax) is characterized by enormous plasticity and according to morphology and feeding strategy, different mastax types can be distinguished. The cuticular hard parts (trophi) of the mastax are often highly specialized and have both a major taxonomic and phylogenetic relevance. Owing to numerous light and scanning electron microscopic studies, the morphology of the trophi is well known but only few attempts have been made to analyze the morphology and functionality of the mastax as a whole. Particularly, the complex muscular system connecting the individual trophi elements and moving them against each other was disregarded in the past. Therefore, the subject of the present study is a detailed analysis of the mastax musculature of the proalid rotifer *Bryceella stylata* using a combination of transmission electron and confocal laser scanning microscopic techniques, previously applied for revealing the somatic musculature in rotifers exclusively. Based on ultrathin serial sections and phalloidin-dyed specimens, a total number of six paired and two unpaired individual mastax muscles have been identified for the modified malleate trophi system of *B. stylata*. Possibly homologous muscles in other, so far investigated rotifer species are discussed as well as functional considerations of the individual mastax muscles and their interaction when moving the trophi elements are suggested.

© 2009 Elsevier GmbH. All rights reserved.

Keywords: Rotifera; Proalidae; Mastax; Musculature; Confocal laser scanning microscopy

1. Introduction

Rotifers are a group of aquatic micrometazoans that are most abundant in freshwater habitats but are also present in marine environments as well as in wet mosses and moist soil. With about 2000 described species (Wallace et al. 2006; Segers 2007) they are a remarkably

diverse group characterized by the presence of a complex set of cuticularized jaw elements. These pharyngeal structures, referred to as trophi, are centrally located in the mastax, which is formed by the ventroapical part of the foregut. The trophi elements are being used for food uptake and can be moved against each other by means of muscles spanning between them or between trophi elements and the pharyngeal epithelium. Amongst other shared characters, the pharyngeal jaw elements are one reason why

*Corresponding author. Tel.: +49 441 798 3369.

E-mail address: eike.f.wilts@mail.uni-oldenburg.de (E.F. Wilts).

rotifers (including the non jaw possessing acanthocephalans) together with gnathostomulids and *Limnognathia maerski* have been suggested to constitute the monophyletic taxon Gnathifera (Ahlrichs 1995; Rieger and Tyler 1995; Sørensen 2003) that was recently supported by molecular studies (Witek et al. 2009). Within the group of rotifers the trophi play an important role in species identification and have been one of the most important characters in rotifer systematics, phylogeny and in compiling evolutionary scenarios (Koste 1978; Markevich and Kutikova 1989; Markevich 1993; Sørensen 2002, Riemann et al. 2008a). Therefore, the rotifer mastax and its trophi have been subject of several detailed scanning electron microscopic (SEM) studies during the last decades (e.g. Markevich and Kutikova 1989; Kleinow et al. 1990; Sørensen 2002; Fontaneto et al. 2007). In contrast, only very few investigations on the interaction of trophi and its surrounding musculature, based on histological or ultrathin sections have been carried out so far, most of them in the early 20th century (De Beauchamp 1909; Martini 1912; Seehaus 1930; Stoßberg 1932; Riemann and Ahlrichs 2008). Confocal laser scanning microscopy (CLSM) of whole mount preparations treated with TRITC-conjugated phalloidin was hitherto used to investigate the body musculature of rotifers but, as argued by Riemann and Ahlrichs (2008), failed unraveling the visceral musculature, especially the complex arrangement of mastax musculature, due to limited resolution. Admittedly, CLSM photographs of previous studies dealing with the somatic musculature of rotifers clearly show a complex of distinctly recognizable mastax muscles (Kutikova et al. 2001, 2006; Sørensen et al. 2003; Santo et al. 2005; Hochberg and Gurbuz 2007, 2008; Riemann et al. 2008b, Wilts et al. 2009), although these were not analyzed in detail. In fact, it is difficult to follow the architecture of the complex mastax musculature on the basis of CLSM data sets exclusively, because insertion of the visceral muscles can only be assumed. Moreover, in a visceral position fluorescent-phalloidin can stain glands and protonephridia containing F-actin (Leasi and Todaro 2008) and possibly nerves (Hochberg and Litvaitis 2000) as well. For avoiding any doubt about nature, position and insertion of the muscular fibers, we applied a combination of both techniques, CLSM and TEM, that, however, were never used together before to unravel the morphology of the muscles being attached to the trophi. The subject matter of our study was the cosmopolitan rotifer *Bryceella stylata* (Milne, 1886). The small proalid species mainly lives in moist terrestrial habitats like mosses and leaf-litter but also occurs in acidic waters, gliding on the substrate or on detritus particles and feeding on small diatoms, presenting a mastax type designated as modified malleate. *B. stylata* was chosen for this study for different reasons: (a) With the successful mastax

musculature reconstruction in a species that small (mastax length of *B. stylata*: ~20 µm), we show that CLSM is a very useful technique and principally suitable for revealing the mastax musculature in all rotifer species, independently from their size and (b) the revealed results are supposed to be valuable for future phylogenetic analyses of the mastax musculature and will hopefully contribute solving the phylogenetic position of *Bryceella* within monogonont rotifers.

The CLSM data sets of the mastax region of four individuals give a good overview of the relative position of the muscle fibers to each other and the trophi elements. Ultrathin serial sections, being observed under the TEM, document the ultrastructure of the individual muscle fibers, their points of insertion on the trophi elements as well as their direction of tension. Combining the 3-dimensional visualization of distinctly stained individual mastax muscles presented by CLSM with the high resolution of TEM on subcellular level, is a useful method to analyze the complex mastax musculature with the advantages of both microscopical techniques.

2. Material and methods

Specimens of *B. stylata* were sampled in wetland mosses taken from a forest near Leer, North-west Germany (53°15'48.14"N, 7°31'54.46"E) in January 2007. Individual specimens were isolated from the samples under a stereomicroscope and studied by transmission electron microscopy (Zeiss EM 902A) as well as confocal laser scanning microscopy (Leica TCS SP 5). Trophi were prepared under a stereomicroscope (Leica MZ12.5) generally following the procedure of De Smet (1998) but with SDS/DTT (modified after Kleinow et al. 1990) as the dissolving agent. The trophi were studied using a scanning electron microscope (Zeiss DSM 940). For transmission electron microscopy, specimens were anaesthetized for 2 min in an aqueous solution of 0.25% bupivacaine (Bucain[®]) and subsequently fixed with 1% OsO₄ in 0.1 M sodium cacodylate buffer at 6 °C. After fixation, specimens were dehydrated in an increasing acetone series, embedded in Araldite, hardened at 60 °C for 72 h and ultrasectioned (75 nm) on a Reichert ultracut E followed by automatic staining with uranyl acetate and lead citrate (Leica EM Stain). The ultrathin cross sections were viewed with a Zeiss EM 902 A at 80 kv and photographed with a Dual Scan CCD camera using the multiple image alignment (MIA) function of ITEM[®] software (Soft Imaging System, Olympus, Münster, Germany). For confocal laser scanning microscopy specimens were placed in a drop of freshwater and relaxed in a 0.25% solution of bupivacaine at 8 °C. The anaesthetised specimens were

fixed for 1 h in phosphate-buffered 4% paraformaldehyde and rinsed in PBS, made permeable by exposure to 0.1% Triton X-100 buffered in 0.1 M PBS for 1 h. For staining, 2 μ l of a 38 μ M methanolic TRITC-labelled phalloidin solution were added to 100 μ l of 0.1% Triton X-100 buffered in 0.1 M PBS. Several specimens were stained for 3 h and mounted in Citifluor[®] on a microscopic slide sealed with a cover slip. Totally, three specimens were analyzed. The images were taken under wavelength of 488 nm, obtained with a Leica TCS SP 5 confocal laser scanning microscope. We used Leica[®] LAS AF 1.7.0 and Amira[®] 5.1 for analysis of the image stacks. Illustrations were carried out with Adobe Illustrator[®] CS2.

3. Results

3.1. General organization of the mastax of *B. stylata*

The bilateral symmetrical mastax complex of the dorsoventrally flattened species *B. stylata* is located ventrally in the neck and anterior trunk region. It comprises epithelial cells, salivary glands, distinct individual muscles, sensory cilia and a system of extracellular trophi elements that is designated as modified malleate. The so called incus is composed of the unpaired fulcrum and the paired rami (Fig. 1A, B). The paired unci (Fig. 1A, B) and manubria (Fig. 1A, B) together form the malleus. The seven main elements of the jaw apparatus are supplemented by an unpaired hypopharynx (Fig. 1A, B) and a subuncinal structure (Fig. 1A, B) located ventral to the uncus (referred to as distal subuncus). The cuticularized trophi elements are embedded in epithelial tissue, from which cells extend

into the cuticular cavities of the rami (ramus basal and ramus subbasal chambers) and manubria (dorsal, median and ventral manubrial chambers) (Fig. 1A). For a detailed description of the individual trophi elements of *B. stylata* see Wilts et al. (2009).

3.2. Muscular system of the mastax of *B. stylata*

The mastax of *B. stylata* displays an antagonistic system of individual, distinct cross-striated, bilaterally symmetrical muscles. Within the muscle cells a large number of mitochondria is visible in direct proximity to the myofibrils. In total, our study has revealed six paired and two unpaired muscles that are attached to the trophi. All muscles either connect trophi elements or trophi elements and epithelial tissue of the mastax or the pharyngeal wall. TEM observations demonstrate that muscle cells and trophi elements are interconnected via hemidesmosomes and tonofilaments across a thin layer of epithelial tissue. Visualized with CLSM and on ultrathin sections the cross-striation of the muscles is more or less distinctly visible. Making it easier to figure out the relative position of the individual mastax muscles to the different trophi elements, we provide CLSM figures of two different specimens: Fig. 2 compares transmission light with fluorescence laser channel images and Fig. 3 displays the CLSM data of a second, completely planar orientated specimen.

In the following, the mastax muscles are described in order of their appearance from dorsal to ventral, except for the musculus circumglandis that enfolds the manubria and salivary glands in dorsoventral direction. For clarity, the hypopharyngeal element, located ventral to the rami (Fig. 1A, B), was excluded from the diagrammatic overview of the muscles (Fig. 4).

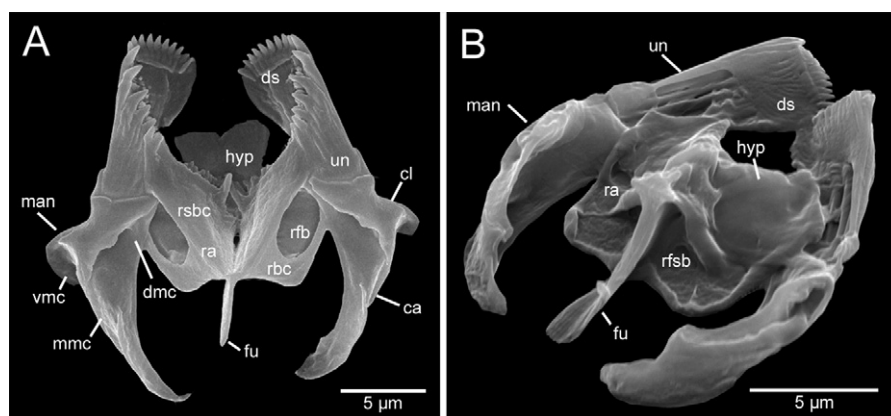


Fig. 1. SEM images of the trophi of *Bryceella stylata*. (A) In dorsal view; (B) in ventrocaudal view. ca = cauda, cl = clava, ds = distal subuncus, dmc = dorsal manubrial chamber, fu = fulcrum, hyp = hypopharynx, man = manubrium, mmc = median manubrial chamber, ra = ramus, rbc = ramus basal chamber, rfb = ramus foramen basal, rfsb = ramus foramen subbasalis, rsbc = ramus subbasal chamber, un = uncus, vmc = ventral manubrial chamber.

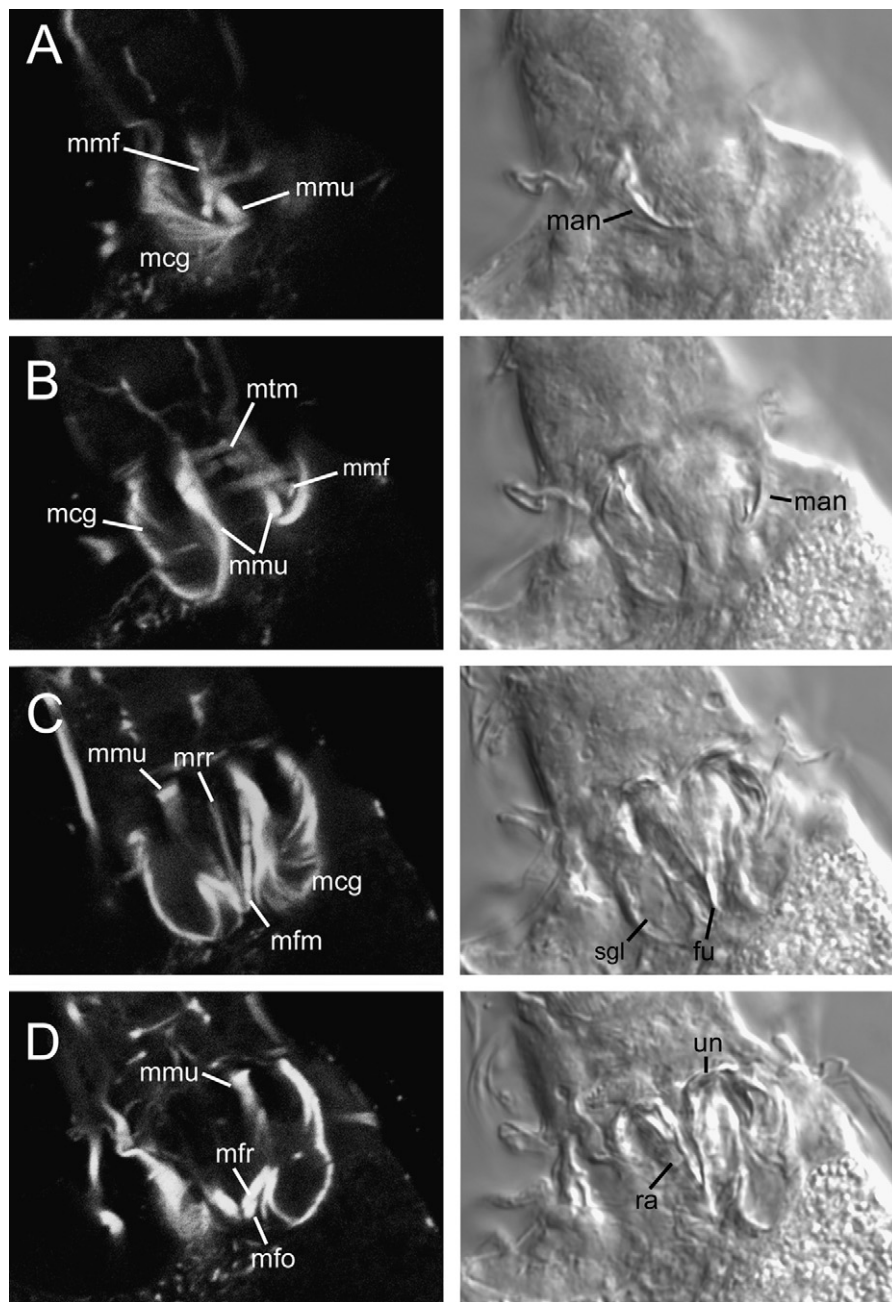


Fig. 2. CLSM series of mastax musculature of *Bryceella stylata* and parallel light microscopic images from dorsal to ventral (A–D). fu = fulcrum, man = manubrium, mcg = musculus circumglandis, mfm = musculus fulcro-manubricus, mfo = musculus fulcro-oralis, mfr = musculus fulcro-ramicus, mmf = musculus manubrico-frontalis, mmu = musculus manubrico-uncus, mrr = mastax receptor retractor, mtm = musculus transversus manubrii, ra = ramus, sgl = salivary gland, un = uncus.

Musculus manubrico-frontalis (mmf) (Figs. 2A, B, 3A, 4A and 5A–D). This dorsalmost paired mastax muscle expands with an inwardly curved course from the posterior region of the cauda (Figs. 2A, B, 5B and 6A) to a point in the direct proximity of the manubrium–uncus joint (Fig. 5A). The muscle is $\sim 10 \mu\text{m}$ long and has a diameter of $\sim 1.3 \mu\text{m}$ in cross section at the point of attachment to the cauda. Unfortunately, neither the

CLSM images nor the ultrathin sections allow an exact determination of whether the muscle inserts with its frontal end on the manubrium and the uncus or if it simply terminates dorsally in the pharyngeal wall.

Musculus transversus manubrii (mtm) (Figs. 2B, 3A and 4B). The unpaired muscle is formed by three bundles of contractile fibers that interconnect the manubrial clavae dorsally (Fig. 5C, D and 6A) and

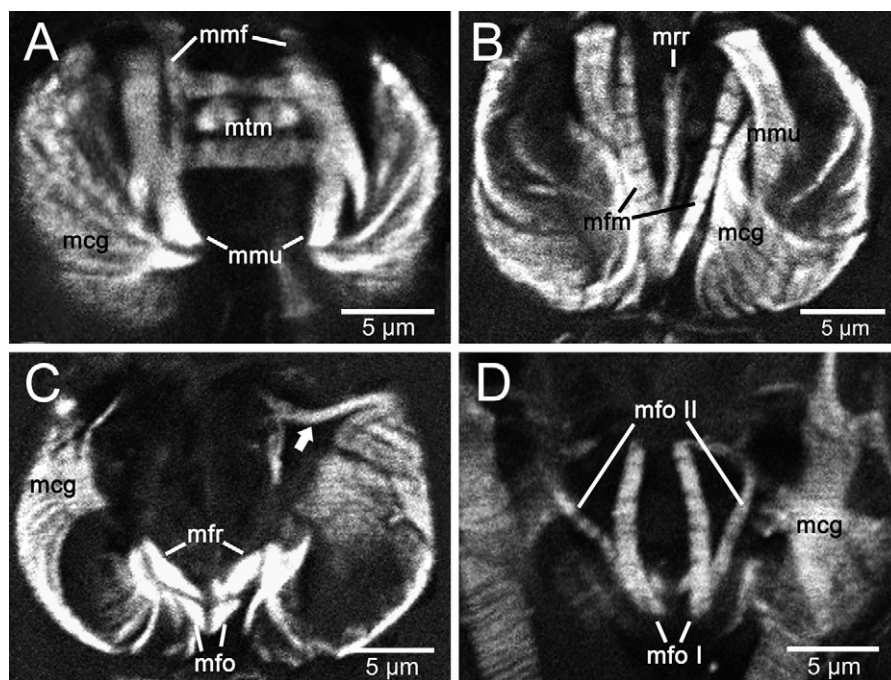


Fig. 3. CLSM series of the mastax musculature in *Bryceella stylata*, optical sections from dorsal to ventral (A–D). mcg = musculus circumglandis, mfm = musculus fulcro-manubricus, mfo I–II = musculus fulcro-oralis I–II, mfr = musculus fulcro-ramicus, mmf = musculus manubrico-frontalis, mmu = musculus manubrico-uncus, mrr = mastax receptor retractor, mtm = musculus transversus manubrii. Arrow (connection between musculus circumglandis and distal subuncus).

has a length of $\sim 16 \mu\text{m}$. The three bundles of this muscle are distinctly separated from each other, whereas the median bundle shows an interruption medially. All three bundles together show an anteroposterior width of $\sim 5 \mu\text{m}$.

Musculus manubrico-uncus (mmu) (Figs. 2A–D, 3A, B and 4C). This paired muscle represents the strongest mastax muscle. Its fibers connect the inner surface of the uncus teeth (Fig. 5C) with the inner surface of the manubrial caudae (Fig. 5E, F) over a length of $\sim 11 \mu\text{m}$. In cross section the muscle appears oval to rectangular.

Musculus fulcro-manubricus (mfm) (Figs. 2C, 3B and 4D). This paired muscle is attached to the inner, dorsal margin of the manubrial clavae in proximity of the manubria-unci joints (Figs. 5C and 7A) and distally to the dorsolateral ends of the fulcrum (Figs. 6B and 7B). Along its course the muscle crosses the musculus manubrico-uncus frontally (see Fig. 3B and compare Fig. 4C with 4D) and runs above the rami (Figs. 6A and 7C). The muscle measures $\sim 15 \mu\text{m}$ in length and shows a diameter of $1.3 \mu\text{m}$ in cross section where attached to the fulcrum.

Mastax receptor retractor (mrr) (Figs. 2C, 3B and 4E). This inconspicuous, unpaired muscle is attached to the dorsal edge of the fulcrum (Figs. 6B and 7B) from where it runs frontally along the median axis of the mastax and terminates in the mastax receptor (Fig. 7C). It has a length of $\sim 12 \mu\text{m}$ and a diameter of $\sim 0.8 \mu\text{m}$

near the fulcrum. For a detailed description of the mastax receptor see Clément et al. (1983) and Clément (1987).

Musculus fulcro-ramicus (mfr) (Figs. 2D, 3C and 4F). This conspicuous, paired muscle spans between the fulcrum and the rami. The muscle inserts with its proximal ends at the caudal margins of the ramus basal chambers and stretches caudally over a length of $\sim 5 \mu\text{m}$, with its distal ends being attached to the lateral sides of the fulcrum. In contrast to the narrow fulcrum the muscle appears massive in cross section ($\sim 2.8 \mu\text{m}$) (Figs. 6B and 7B).

Musculus fulcro-oralis (mfo) (Figs. 2D, 3C, D and 4G). This ventralmost, paired muscle consists of two strands each that merge in their posterior region and diverge in its frontal course (compare Fig. 6B with Fig. 7B). Caudally the muscle is attached to the ventrolateral end of the fulcrum. Frontally the longer, exterior branch (musculus fulcro oralis I, length $\sim 11 \mu\text{m}$) and the shorter, interior branch (musculus fulcro oralis II, length $\sim 9 \mu\text{m}$) insert on the epipharyngeal wall. In the proximity of the attachment to the fulcrum the muscle displays a width of $\sim 0.8 \mu\text{m}$ in cross section.

Musculus circumglandis (mcg) (Figs. 2A–C, 3A–D and 4H). This paired muscle consists of a complex network of bundles enveloping the manubria as well as the salivary glands (Figs. 4H and 7D). The muscles are attached to the exterior margin of the manubria from

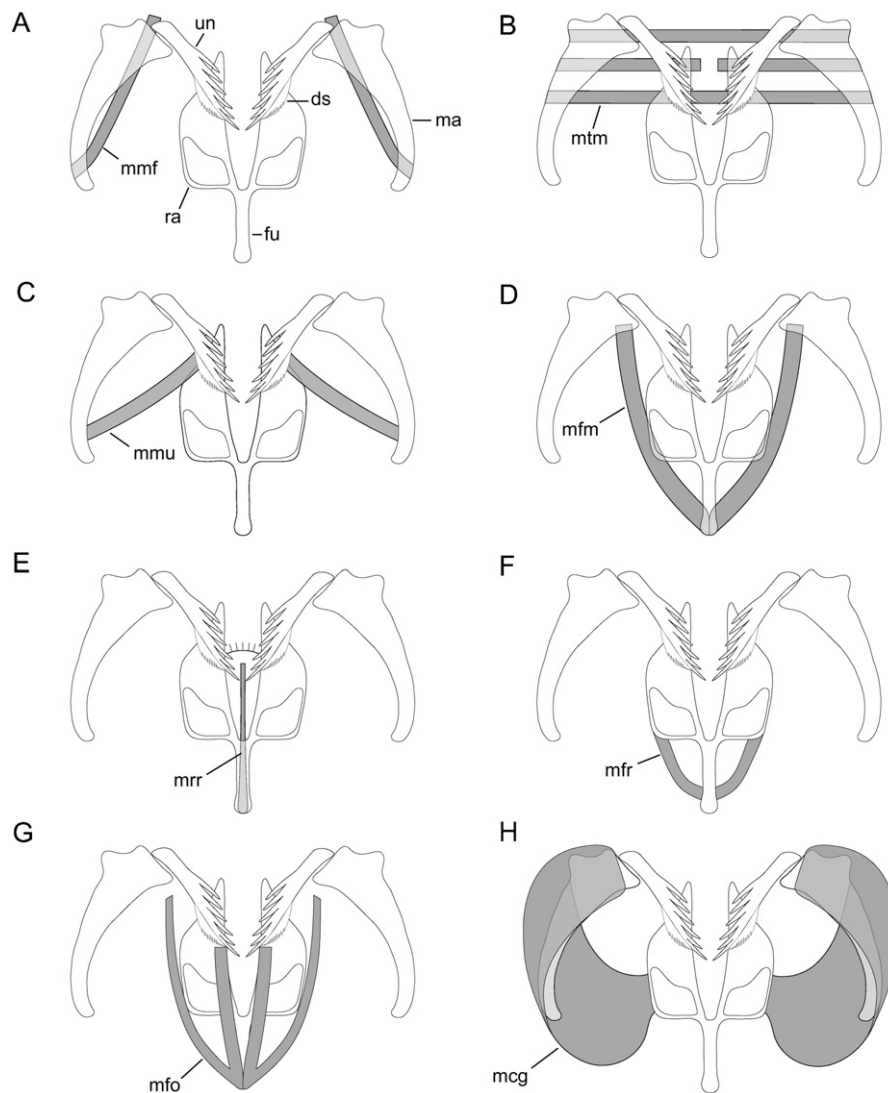


Fig. 4. Mastax musculature in *Bryceella stylata* in ventral view, diagrammatic. The order of musculature (A–H) reflects the appearance of the mastax muscles from dorsal to ventral side. (A) Musculus manubrico-frontalis; (B) musculus transversus manubrii; (C) musculus manubrico-uncus; (D) musculus fulcro-manubricus; (E) mastax receptor retractor; (F) musculus fulcro-ramicus; (G) musculus fulcro-oralis; (H) musculus circumglandis. ds = distal subuncus, fu = fulcrum, ma = manubrium, mcg = musculus circumglandis, mfm = musculus fulco-manubricus, mfo = musculus fulcro-oralis, mfr = musculus fulcro-ramicus, mmf = musculus manubrico-frontalis, mmu = musculus manubrico-uncus, mrr = mastax receptor retractor, mtm = musculus transversus manubrii, ra = ramus, un = uncus.

where they stretch into dorsal and ventral direction. The muscle is also attached to the dorsolateral side of the ramus basal chamber (Figs. 6A and 7C). Moreover, the ultrathin sections display a connection between the musculus circumglandis and the subuncus (arrows in Figs. 5D and 6A). On the basis of the TEM images it could not be figured out if the connection is realized by contractile material of the muscle. However, on CLSM images a branch running off the anterior region of the musculus circumglandis is clearly visible (arrow Fig. 3C). The maximum frontocaudal extension measures ~18 µm; its dorsoventral extension measures ~11 µm.

4. Discussion

4.1. Mastax musculature within Rotifera

The obvious cross-striation of the visceral mastax musculature is documented in previous light and electron microscopic studies (De Beauchamp 1909; Martini 1912; Nachtwey 1925; Remane 1929–1933; Stoßberg 1932; Riemann and Ahlrichs 2008) as well as in confocal microscopic analyses (Sørensen et al. 2003; Santo et al. 2005; Kotikova et al. 2006; Hochberg and Gurbuz 2008; Wilts et al. 2009). The cross-striation of

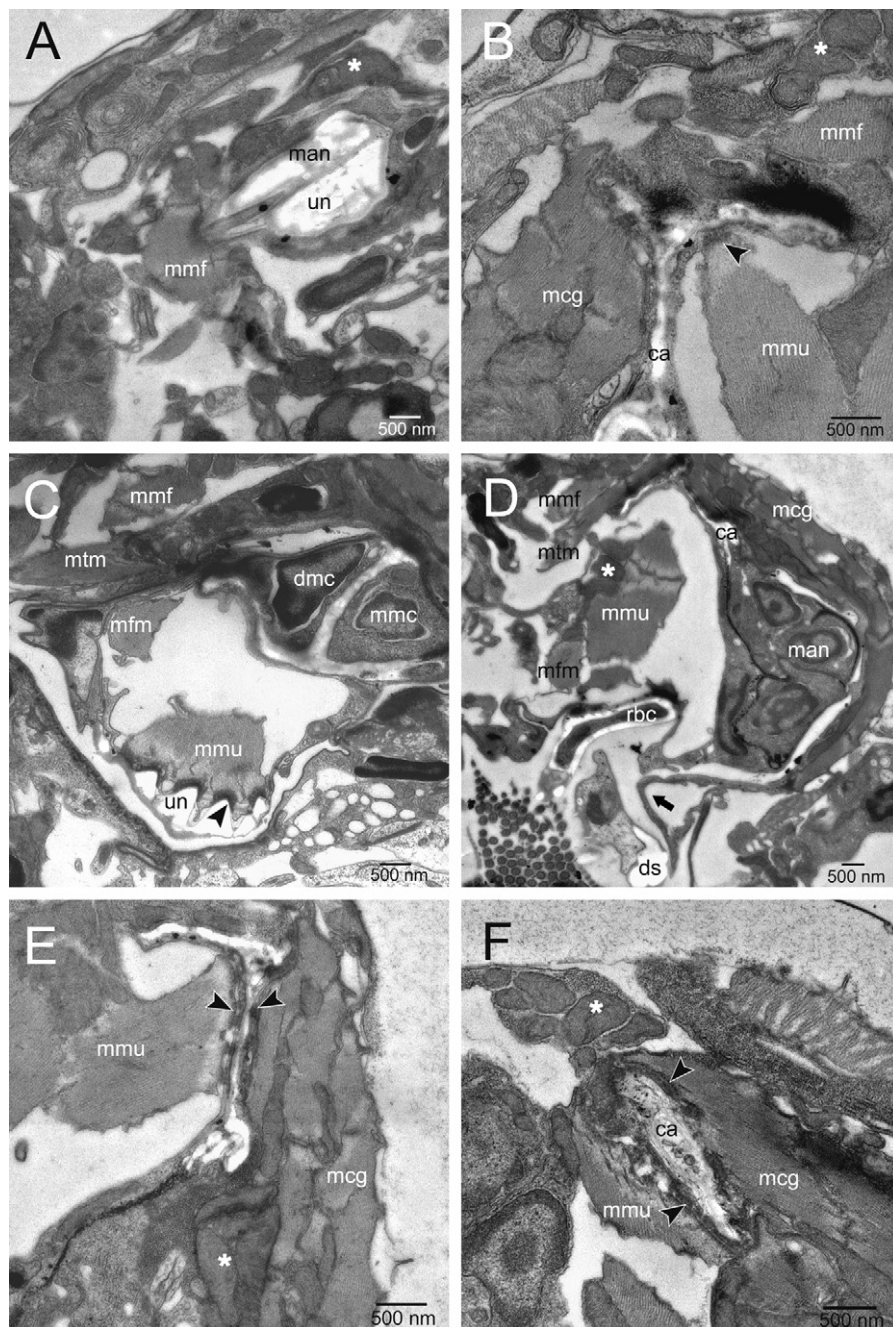


Fig. 5. TEM images of selected details of the mastax of *Bryceella stylata* in cross section. (A) Musculus manubrico-frontalis in the proximity of its anterior end; (B) musculus manubrico-frontalis in the proximity of its insertion on the cauda; (C) musculus manubrico-uncus with attachment to the uncus; (D) musculus manubrico-uncus stretching above the rami; (E) musculus manubrico-uncus with insertion on the posterior region of the cauda; (F) terminal end of the cauda with insertion of musculus manubrico-uncus and musculus circumglandis. ca = cauda, dmc = dorsal manubrial chamber, ds = distal subuncus, man = manubrium, mcg = musculus circumglandis, mmc = median manubrial chamber, mmf = musculus manubrico-frontalis, mmu = musculus manubrico-uncus, mtm = musculus transversus manubrii, rbc = ramus basal chamber, un = uncus. Arrow heads (hemidesmosomes), arrow (connection between musculus circumglandis and distal subuncus), asterisks (mitochondria).

the myofibrils can be used to identify the direction of tension of the muscles.

B. stylata displays a muscle that connects the cauda with the anterior pharyngeal wall (musculus manubrico-frontalis, Fig. 4A). De Beauchamp (1909) demonstrated

the presence of a paired muscle connecting the cauda with the uncus (musculus extensor mallei) in the virgate, forcipate and malleate mastax types and suggested it to affect a spread of the malleus. In *Notholca acuminata* a similar muscle has been identified by Sørensen et al.

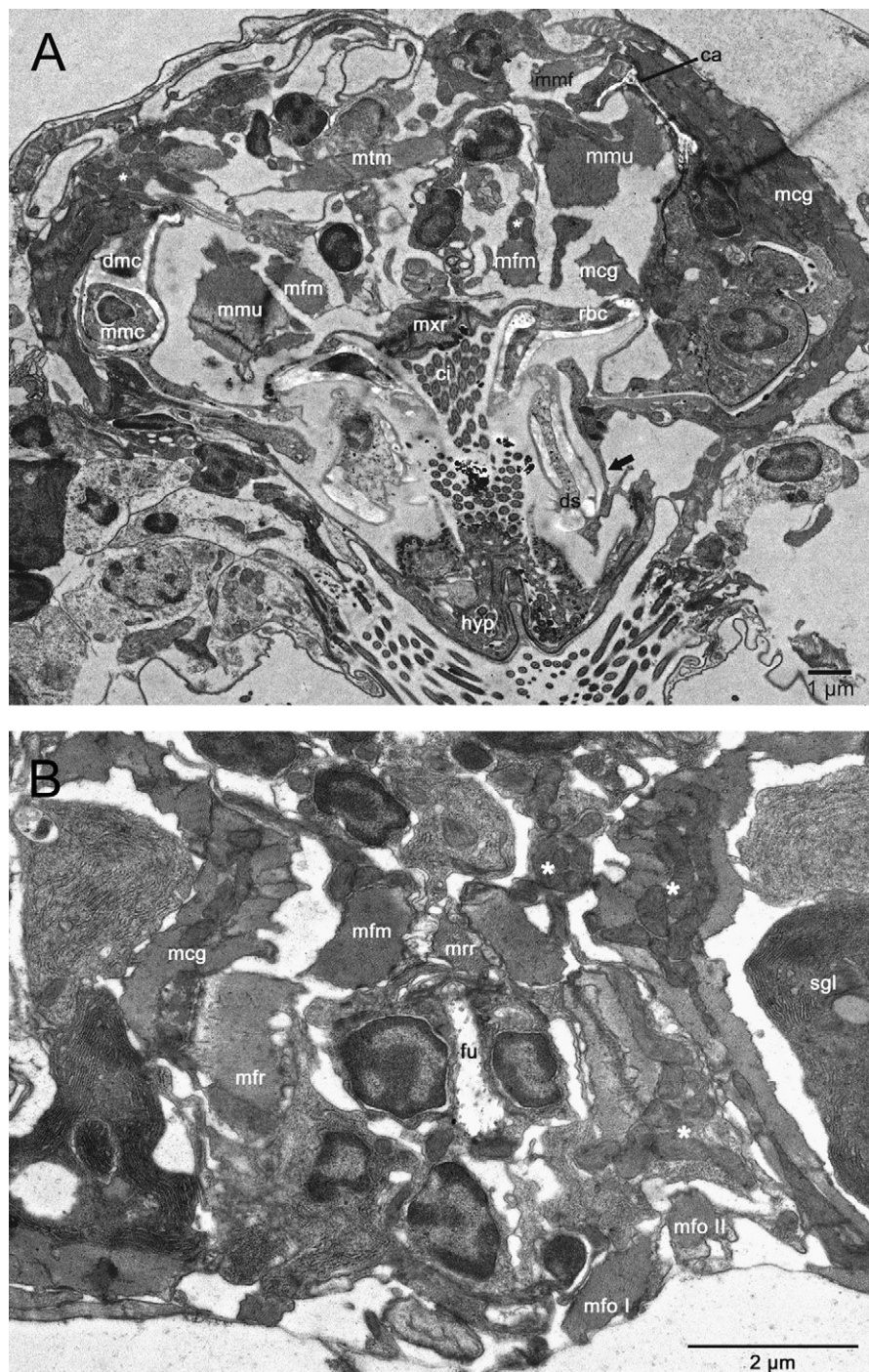


Fig. 6. TEM images of cross sections of *Bryceella stylata*. (A) Median mastax region; (B) fulcrum region; ca = cauda, ci = cilia, dmc = dorsal manubrial chamber, ds = distal subuncus, fu = fulcrum, hyp = hypopharynx, mcg = musculus circumglandis, mfm = musculus fulcro-manubricus, mfo I, II = musculus fulcro-oralis I, II, mfr = musculus fulcro-ramics, mmc = median manubrial chamber, mmf = musculus manubrico-frontalis, mmu = musculus manubrico-uncus, mrr = mastax receptor retractor, mtm = musculus transversus manubrii, mxr = mastax receptor, rbc = ramus basal chamber, sgl = salivary gland. Arrow (connection between musculus circumglandis and distal subuncus), asterisks (mitochondria).

(2003) (mallei flexors). However, the presence of a muscle like the musculus manubrico-frontalis in a forcipate mastax could not be verified with the data of Riemann and Ahlrichs (2008) who did not record it in

Dicranophorus forcipatus. After De Beauchamp (1909) the musculus extensor mallei in *Epiphanes senta* connects the cauda with the anterior pharyngeal wall but an attachment to the uncus could not be verified just

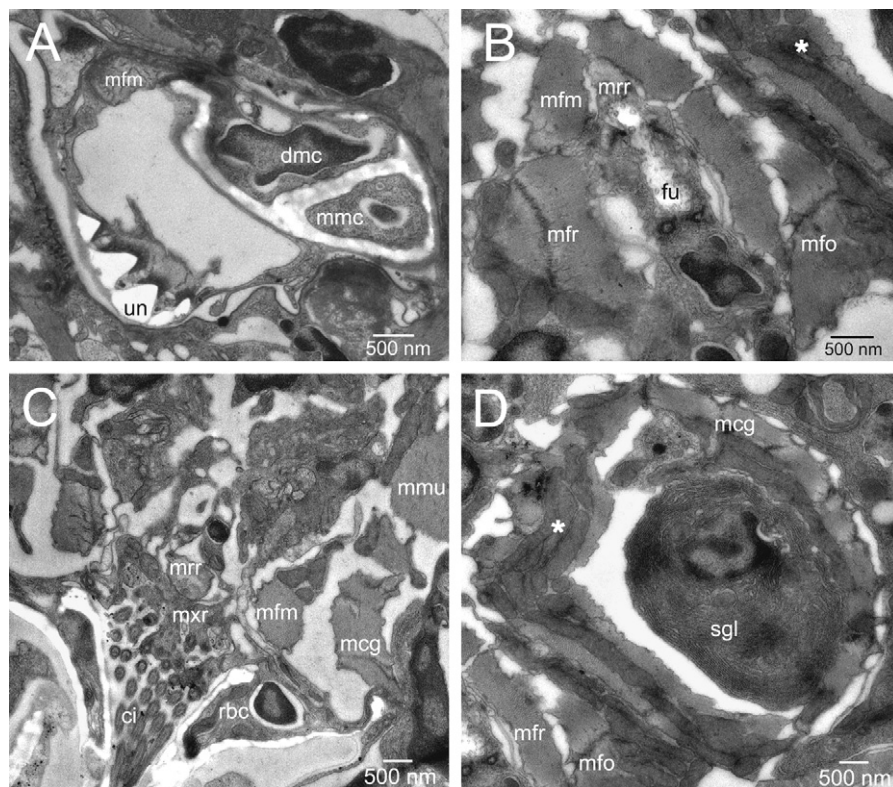


Fig. 7. TEM images of selected details of the mastax of *Bryceella stylata* in cross section. (A) Attachment of musculus fulcro-manubricus to the clava; (B) musculus fulcro-manubricus, musculus fulcro-ramicus, musculus fulcro-oralis and mastax receptor retractor in the proximity of the fulcrum; (C) section through rami and mastax receptor; (D) posterior region of salivary gland encircled by musculus circumglandis. ci = cilia, dmc = dorsal manubrial chamber, fu = fulcrum, mcg = musculus circumglandis, mfm = musculus fulcro-manubricus, mfo = musculus fulcro-oralis, mfr = musculus fulcro-ramicus, mmc = median manubrial chamber, mmu = musculus manubrico-uncus, mrr = mastax receptor retractor, mxr = mastax receptor, rbc = ramus basal chamber, sgl = salivary gland, un = uncus. Asterisks (mitochondria).

like in *B. stylata*. Without further data on the mastax musculature of different rotifer species, a hypothesis on the homology of the musculus manubrico-frontalis would be highly speculative.

In *B. stylata* we have found a muscle connecting the clavae of both manubria dorsally (musculus transversus manubrii, Fig. 4B). As seen on CLSM images, this muscle seems also to be present in *Brachionus urceolaris* (see Fig. 1C, F in Santo et al. 2005) and *Euchlanis dilatata unisetata* (see Fig. 6A in Kotikova et al. 2001) and comprises, like the musculus transversus manubrii in *B. stylata*, more than one distinct fiber. A musculus transversus manubrii was also stated for *D. forcipatus* by Riemann and Ahlrichs (2008) only comprising a single, broad muscle fiber. Probably the musculus transversus manubrii provides a stabilization of the mallei and an approaching of the clavae when contracting. Considering the same position of the muscle in *B. stylata*, *Brachionus urceolaris*, *Euchlanis dilatata unisetata* and *D. forcipatus* a homology seems to be plausible.

In *B. stylata* the musculus manubrico-uncus (Fig. 4C), spanning from the manubrial cauda to the inner side of

the uncus, is the strongest of all mastax muscles. Such a muscle has also been documented for *E. senta* (musculus flexor mallei, see Martini 1912); *Euchlanis* (musculus flexor mallei, see Stoßberg 1932) and *D. forcipatus* (musculus manubrico-uncus, see Riemann and Ahlrichs 2008). After Remane (1929–1933) and Stoßberg (1932) the musculus flexor mallei effects a grinding movement by deflection of the manubrium–uncus joint with an approach of the uncus towards the manubrium, since the manubrium is stabilized by other mastax muscles. The above described muscles (mmu) in *Epiphanes*, *Euchlanis*, *Dicranophorus* and *Bryceella* are considered to be homologous due to their identical positions and starting points.

Like the musculus fulcro-manubricus in *B. stylata* (Fig. 4D) a paired muscle, spanning between the laterocaudal fulcrum end and the dorsal border of the manubrial clava, has also been observed in *E. senta* (processus posterior, see Martini 1912), *Euchlanis* (musculus fulcro-manubricus, see Stoßberg 1932), *N. acuminata* (musculus fulcro-manubricus, see Sørensen et al. 2003), and *D. forcipatus* (musculus

fulcro-manubricus, see Riemann and Ahlrichs 2008). The musculus fulcro-manubricus probably acts as an antagonist to the musculus manubrico-uncus by drawing back the clava and extending the angle of the manubrium–uncus joint. Because of the position and function, we assume a homology of the corresponding muscles of the above mentioned species.

In *B. stylata*, we found a muscle that connects the dorsocaudal end of the fulcrum and the mastax receptor (mastax receptor retractor, Fig. 4E). A similar muscle has been observed in *Synchaeta pectinata* (muscle dépresseuse de piston, see De Beauchamp 1909), *Trichocerca bicristata* (muscle dépresseuse de piston, see De Beauchamp 1909), *Notommata copeus* (muscle dépresseuse de piston, see De Beauchamp 1909), *E. senta* (musculus fulcro-mucosus, compare Martini 1912 and Remane 1929–1933), *Euchlanis* (musculus fulcro-mucosus, see Stoßberg 1932) and *D. forcipatus* (mastax receptor retractor, see Riemann and Ahlrichs 2008). The muscle appears unpaired in all species listed above except in *S. pectinata* and *T. bicristata* that both possess a virgate mastax. For *N. copeus* the situation is unclear. Martini (1912) and Stoßberg (1932) suppose that this muscle, also referred to as hypopharyngeal muscle or piston, effects an expansion of the mastax lumen with its contraction. Following Stoßberg (1932) and Remane (1929–1933) its functions, especially in the virgate mastax, as a piston enabling a sucking function. A lack of this muscle was proposed for the forcipate mastax by Remane (1929–1933) but this hypothesis was falsified by Riemann and Ahlrichs (2008) who detected the muscle in *D. forcipatus*. For the Proalidae, the hypopharyngeal muscle was stated to be attached caudally on the pharyngeal wall and not on the fulcrum. This criterion was previously used as a diagnostic character for Proalidae (see Koste 1978 and De Smet 1996). However, with the finding in *B. stylata*, where the mastax receptor retractor is definitely attached to the fulcrum, this diagnostic character is no longer valid. It is plausible, that this muscle, connecting the fulcrum and the mastax receptor, is homologous in all species where it has been identified. Furthermore, due to its wide distribution across Rotifera, we assume it to be a ground pattern feature at least in Ploima.

B. stylata shares the presence of a muscle connecting the fulcrum and the rami (musculus fulcro-ramicus, Fig. 4F) with different rotiferan taxa including *E. senta* (musculus fulcroscapalis, see Martini 1912), *Euchlanis* (musculus fulcroscapalis, see Stoßberg 1932 and abducteur horizontal, see De Beauchamp 1909), *Testudinella patina* (musculus abductor rami, see Seehaus 1930), *N. acuminata* (musculus fulcro-scapalis, see Sørensen et al. 2003) and *D. forcipatus* (musculus fulcro-ramicus, see Riemann and Ahlrichs 2008). De Beauchamp (1909) described a muscle connecting the fulcrum with the rami even for the uncinata (see Fig. LII in De Beauchamp 1909) and the incudate

mastax type (see Fig. L in De Beauchamp 1909). Remane (1929–1933), who abstracted the results of De Beauchamp, refers to this muscle as musculus abductor rami. The musculus fulcro-ramicus is assumed to realize an opening of the rami with its contraction. Due to the function, position and distribution of the above mentioned muscles among the listed species, these muscles can reasonably assumed to be homologous. Moreover, according to the existing data on the presence of the musculus fulcro-ramicus in Epiphanidae, Euchlanidae, Brachionidae, Dicranophoridae, Proalidae and Gnesiotrocha (Testudinellidae and Collothecaceae), this muscle is a possible ground pattern feature for Monogononta (see also Riemann and Ahlrichs 2008).

B. stylata possesses a paired, bifurcating muscle that spans ventrally between the distal end of the fulcrum and the anterior pharyngeal wall (musculus fulcro-oralis, Fig. 4G). This muscle is also present in *E. senta* (musculus fulcro-oralis; Martini 1912). Following Martini (1912), this muscle effects a widening of the mouth opening. A paired, ventral muscle (musculus hypopharyngeus) was found in *D. forcipatus* by Riemann and Ahlrichs (2008) but in contrast to the muscles in *B. stylata* and *E. senta*, the musculus hypopharyngeus connects the distal fulcrum end with the hypopharyngeal plates. According to course and shape, we assume a homology of the musculus fulcro-oralis in *B. stylata* and *E. senta*, whereas the homology with the musculus hypopharyngeus in *D. forcipatus* is unclear.

In *B. stylata*, a paired muscle connects the manubrial caudae with the posterior part of the rami (musculus circumglandis, Fig. 4H). The posterior part of the musculus circumglandis runs from the inner dorsal side of the cauda to the dorsal surface of the ramus subbasal chamber. Furthermore, the musculus circumglandis almost completely envelopes the manubria and the salivary glands, that are possibly compressed with contraction of the muscle. A muscle like the musculus circumglandis has been documented in *Euchlanis* (musculus ramo-manubricus, see Stoßberg 1932) and *N. acuminata* (caudae abductors, see Sørensen et al. 2003). A muscle of possible similar function was found in *D. forcipatus* (musculus circumglandis, see Riemann and Ahlrichs 2008), apparently connecting the posterior part of the caudae with the fulcrum while encircling the salivary glands. Possibly, the musculus circumglandis of *B. stylata* possesses the same function (spread of the rami) like the musculus ramo-manubricus in *Euchlanis* and caudae abductors in *N. acuminata*. According to its course and shape, the musculus circumglandis in *B. stylata* is unique in its shape among the so far investigated rotifer species. A conclusion concerning the homology of the musculus circumglandis of *B. stylata* with muscles in the listed species currently remains uncertain.

A summary of our hypotheses on the homology of the individual mastax muscles is presented in Table 1. This

Table 1. Mastax muscles of *Bryceella stylata* and their homologous synonyms in other thus far investigated rotifers. + indicates the presence of the individual mastax muscle; synonymous terms in brackets and (+) indicate insecure homology.

	<i>Bryceella stylata</i>	<i>Epiphanes senta</i>	<i>Euchlanis dilatata</i>	<i>Notholca acuminata</i>	<i>Brachionus urceolaris</i>	<i>Testudinella patina</i>	<i>Synchaeta pectinata</i>	<i>Trichocerca bicristata</i>	<i>Notommata copeus</i>	<i>Dicranophorus forcipatus</i>
Mastax type	modified malleate	malleate	malleate	malleate	malleate	malleoramate	virgate	virgate	virgate	forcipate
Musculus										
manubrico-frontalis	+	extensor mallei		mallei flexors						
transversus manubrii	+		+ ^{***}		+					+
manubrico-uncus	+	flexor mallei	flexor mallei*							+
fulcro-manubricus	+	processus posterior	+*	+						+
Mastax receptor	+	fulcro-mucosus	fulcro-mucosus*				dépresseur de piston	dépresseur de piston	dépresseur de piston	+
fulcro-ramicus	+	fulcroscapalis	fulcroscapalis*, abducteur horizontal (ramo-manubricus)*	fulcro-scaplis (caudae abductors)		abductor rami				+
circumglandis	+									(+)
fulcro-oralis	+	+								(hypopharyngeus)
Reference	this study	Martini (1912)	De Beauchamp (1909), *Stoßberg (1932), ***Kotikova et al. (2001)	Sørensen et al. (2003)	Santo et al. (2005)	Seehaus (1930)	De Beauchamp (1909)	De Beauchamp (1909)	De Beauchamp (1909)	Riemann and Ahlrichs (2008)

list surely is fragmentary, because we only quote muscles that are definitely recognizable and able to homologize with muscles in *B. stylata* as far as the often incomplete data of previous studies allow. Therefore, it is possible or even likely that we have not identified all muscles of previously examined rotifer species that are homologous with those of *B. stylata*.

4.2. Functional considerations on the trophi movement for food uptake

Based on the reconstruction of the muscular system of the mastax of *B. stylata* and on light microscopic observations of living specimens, we hypothesize the following muscular movements of the trophi as presented in Fig. 8.

The cycle of trophi movements is initiated with the considerable stimulation of the mastax receptor and the simultaneous contraction of the mastax receptor retractor resulting in a widening of the mastax cavity. This activity is supposedly attended by the contraction of the musculus fulcro-oralis that likely either draws the trophi frontally to the mouth opening or widens the mouth

opening towards the trophi. However, the consequence is an approximation of trophi and mouth opening (Fig. 8A). In the next step, the musculus fulcro-ramicus abducts the rami, whereas the unci follow the opening movement passively since both trophi elements are interlocked via ligamentous connections (see Kleinow et al. 1990) (Fig. 8B). Supporting the action of the musculus fulcro-ramicus and providing even more space for incoming food particles, contraction of the musculus fulcro-manubricus causes an extension of the manubrium–uncus joint and is responsible for a backward movement of the malleus relative to the incus (Fig. 8C). Following this opening movement, the contraction of the musculus manubrico-frontalis effects a frontal thrust of the malleus whereby a flexion of the malleus joint and a caudal retraction of the uncus is realized. As a result, the unci teeth push uptaken food particles actively through the rami (Fig. 8D). The previous flexion of the malleus joint is subsequently intensified by narrowing unci and manubrial caudae performed by the musculus manubrico-uncus (Fig. 8E). In the following, the trophi elements carry out a closing movement induced by contraction of the musculus transversus manubrii and relaxation of the musculus fulcro-ramicus. As a result,

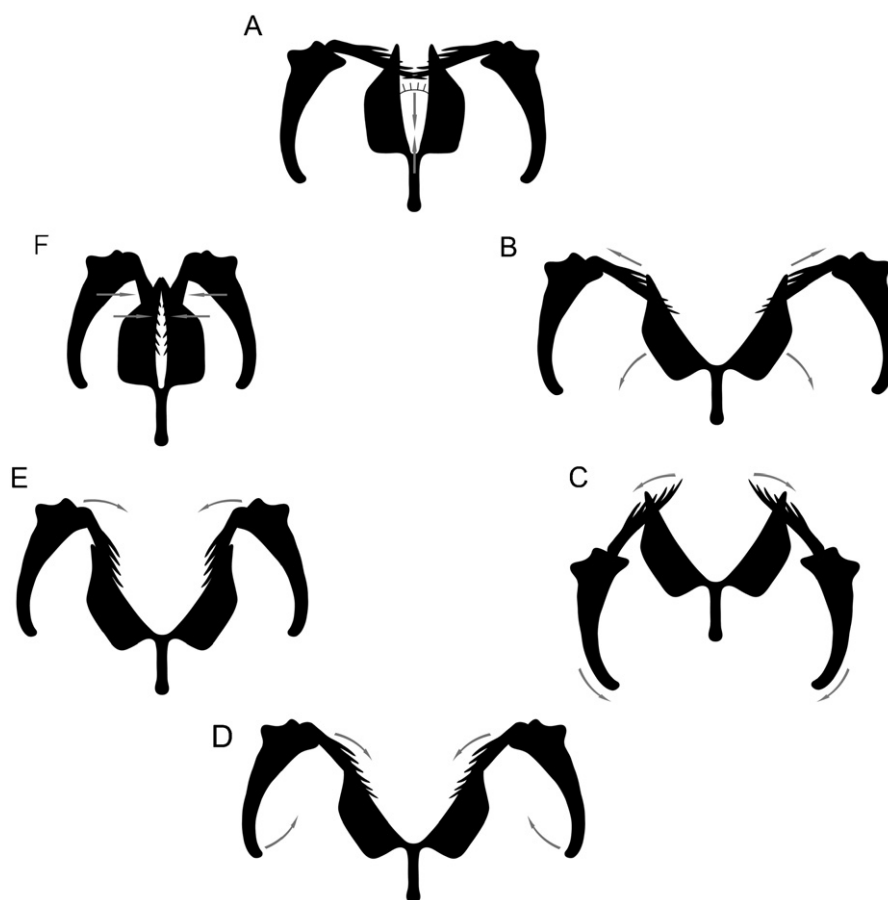


Fig. 8. Diagrammatic overview of movements of trophi elements in *Bryceella stylata* (A–F). Arrows indicate direction of movements of trophi elements realized by mastax musculature.

the manubria are adducted, the unci approach each other, the rami close and food particles are pushed further backwards (Fig. 8F). Possibly this overall closing movement of the trophi is supported by a contraction of the musculus circumglandis that also compresses the salivary glands. As soon as all mastax muscles relax, incus, unci and manubria return to their original position and a new cycle of muscular activity begins. In the absence of stimulation of the mastax receptor, the muscular movement of the trophi ceases.

Although our study on the overall movement of the individual trophi elements presents a plausible hypothesis, we are not able to provide the exact order in which individual mastax muscles relax.

4.3. Conclusion

With this study we hope to introduce the combination of CLSM and TEM and demonstrate its usefulness when revealing the complex arrangement of rotiferan mastax musculature. From future studies dealing with the musculature of the different mastax types, we expect new insights into morphology, functionality and evolution of the mastax and hope its musculature to be another helpful tool for revealing rotifer phylogeny. However, before being able to use the mastax musculature as a phylogeny-informative character system, homology of each muscle has to be identified thoroughly.

Acknowledgements

We gratefully acknowledge financial support granted to E.F. Wilts by the Evangelisches Studienwerk Villigst. Support was also provided by Deutsche Forschungsgemeinschaft DFG. We thank Prof. Dr. P. Martínez Arbizu from Senckenberg Research Institute, German Centre for Marine Biodiversity Research (DZMB), for providing the confocal laser scanning microscope. Moreover, valuable comments and remarks on this manuscript provided by M. V. Sørensen, F. Leasi and A. Kieneke are much appreciated.

References

- Ahlrichs, W.H., 1995. In: *Ultrastruktur und Phylogenie von Seison nebaliae* (Grube 1859) und *Seison annulatus* (Claus 1876). Cuvillier Verlag, Göttingen 310 pp.
- Clément, P., Wurdak, E., Amsellem, J., 1983. Behavior and ultrastructure in rotifers. *Hydrobiologia* 104, 89–130.
- Clément, P., 1987. Movements in rotifers: correlations of ultrastructure and behavior. *Hydrobiologia* 147, 339–359.
- De Beauchamp, P., 1909. Recherches sur les Rotifères: Les formations tégumentaires et l'appareil digestif. *Arch. Zool. Exp. Paris* 10, 1–410.
- De Smet, W.H., 1998. Preparation of rotifer trophi for light and scanning electron microscopy. *Hydrobiologia* 387–388, 117–121.
- De Smet, W.H., 1996. Rotifera 4: the Proalidae (Monogononta). In: Dumont, H.J., Nogrady, T. (Eds.), *Guides to the Identification of the Microinvertebrates of the Continental Waters of the World*. SPB Academic Publishing BV, Amsterdam, pp. 1–102.
- Fontaneto, D., Herniou, E.A., Boschetti, C., Caprioli, M., Melone, G., Ricci, C., Barraclough, T.G., 2007. Independently evolving species in asexual bdelloid rotifers. *Plos. Biol.* 5 (4), e87, doi:10.1371/journal.pbio.0050087.
- Hochberg, R., Litvaitis, M.K., 2000. Functional morphology of the muscles in *Philoina* sp. (Rotifera: Bdelloidea). *Hydrobiologia* 432, 57–64.
- Hochberg, R., Gurbuz, O.A., 2007. Functional morphology of somatic muscles and anterolateral setae in *Filinia novaezealandiae* Shiel and Sanoamuang, 1993 (Rotifera). *Zool. Anz.* 246, 11–22.
- Hochberg, R., Gurbuz, O.A., 2008. Comparative morphology of the somatic musculature in species of *Hexarthra* and *Polyarthra* (Rotifera, Monogononta): its function in appendage movement and escape behavior. *Zool. Anz.* 247, 233–248.
- Kleinow, W., Klusemann, J., Wratil, H., 1990. A gentle method for the preparation of hard parts (trophi) of the mastax of rotifers and scanning electron microscopy of the trophi of *Brachionus plicatilis* (Rotifera). *Zoomorphology* 109, 329–336.
- Koste, W., 1978. In: *Rotatoria. Die Rädertiere Mitteleuropas. Ein Bestimmungswerk, begründet von Max Voigt. Ueberordnung Monogononta, second ed. I. Textband*. Gebrüder Borntraeger Berlin, Stuttgart 673 pp.
- Kotikova, E.A., Raikova, O.J., Flyatchinskaya, L.P., Reuter, M., Gustafsson, M.K.S., 2001. Rotifer muscles as revealed by phalloidin–TRITC staining and confocal scanning laser microscopy. *Acta Zool.* 82, 1–9.
- Kotikova, E.A., Raikova, O.J., Flyatchinskaya, L.P., 2006. Study of architectonics of rotifer musculature by the method of fluorescence with use of confocal microscopy. *J. Evol. Biochem. Phys.* 42, 89–97.
- Leasi, F., Todaro, M.A., 2008. The muscular system of *Musellifer delamarei* (Renaud-Mornant, 1968) and other chaetonotidans with implications for the phylogeny and systematization of the Paucitubulatina (Gastrotricha). *Biol. J. Linn. Soc.* 94, 379–398.
- Markevich, G.I., 1993. SEM observations on *Seison* and phylogenetic relationships of the Seisonidea (Rotifera). *Hydrobiologia* 255–256, 513–520.
- Markevich, G.I., Kutikova, L.A., 1989. Mastax morphology under SEM and its usefulness in reconstructing rotifer phylogeny and systematics. *Hydrobiologia* 186–187, 285–289.
- Martini, E., 1912. Studien über die Konstanz histologischer Elemente. III. *Hydatina senta*. *Z. Wiss. Zool.* 102, 425–645.
- Nachtwey, R., 1925. Untersuchung über die Keimbahn, Organogenese und Anatomie von *Asplanchna priodonta* Gosse. *Z. Wiss. Zool* 126, 239–492.
- Remane, A., 1929–1933. Rotatoria. In: *Bronn's Klassen und Ordnungen des Tierreichs Bd. 4, Abt. II/1*, pp. 1–577.

- Rieger, R.M., Tyler, S., 1995. Sister-group relationship of Gnathostomulida and Rotifera–Acanthocephala. *Invertebr. Biol.* 114, 186–188.
- Riemann, O., Kieneke, A., Ahlrichs, W.H., 2008a. Phylogeny of Dicranophoridae (Rotifera: Monogononta) – a maximum parsimony analysis based on morphological characters. *J. Zool. Syst. Evol. Res.* 47 (1), 61–76.
- Riemann, O., Ahlrichs, W.H., 2008. Ultrastructure and function of the mastax in *Dicranophorus forcipatus*. *J. Morphol.* 269, 698–712.
- Riemann, O., Martínez Arbizu, P., Kieneke, A., 2008b. Organisation of body musculature in *Encentrum mucronatum* Wulfert, 1936, *Dicranophorus forcipatus* (O.F. Müller, 1786) and in the ground pattern of Ploima (Rotifera: Monogononta). *Zool. Anz.* 247, 133–145.
- Santo, N., Fontaneto, D., Fascio, U., Melone, G., Caprioli, M., 2005. External morphology and muscle arrangement of *Brachionus urceolaris*, *Floscularia ringens*, *Hexarthra mira* and *Notommata glyphura* (Rotifera, Monogononta). *Hydrobiologia* 546, 223–229.
- Seehaus, W., 1930. Zur Morphologie der Rädertiergattung *Testudinella* Bory de St. Vincent. *Z. Wiss. Zool.* 137, 175–273.
- Segers, H., 2007. Annotated checklist of the rotifers (Phylum Rotifera), with notes on nomenclature, taxonomy and distribution. *Zootaxa* 1564, 1–104.
- Sørensen, M.V., 2002. On the evolution and morphology of the rotiferan trophi, with a cladistic analysis of Rotifera. *J. Zool. Syst. Evol. Res.* 40, 129–154.
- Sørensen, M.V., 2003. Further structures in the jaw apparatus of *Limnognathia maerski* (Micrognathozoa), with notes on the phylogeny of the Gnathifera. *J. Morphol.* 255, 131–145.
- Sørensen, M.V., Funch, P., Hooge, M., Tyler, S., 2003. Musculature of *Notholca acuminata* (Rotifera: Ploima: Brachionidae) revealed by confocal scanning laser microscopy. *Invertebr. Biol.* 122, 223–230.
- Stoßberg, K., 1932. Zur Morphologie der Rädertiergattung *Euchlanis*, *Brachionus* und *Rhinoglena*. *Z. Wiss. Zool.* 142, 313–424.
- Wallace, R.L., Snell, T.W., Ricci, C., 2006. Rotifera 1: biology, ecology and systematics. In: Segers, H., Dumont, H.J. (Eds.), *Guides to the Identification of the Microinvertebrates of the Continental Waters of the World* 23 second ed. Kenobi Productions, Academic Publishing, The Hague, The Netherlands, pp. 1–299.
- Witek, A., Herlyn, H., Ebersberger, I., Mark Welch, D.B., Hankeln, T., 2009. Support for the monophyletic origin of Gnathifera from Phylogenomics. *Mol. Phyl. Evol.* 101016/j.ympev.2009.07.031.
- Wilts, E.F., Ahlrichs, W.H., Martínez Arbizu, P., 2009. The somatic musculature of *Bryceella stylata* (Milne, 1886) (Rotifera: Proalidae) as revealed by confocal laser scanning microscopy with additional new data on its trophi and overall morphology. *Zool. Anz.* 248, 161–175.